International Journal of Railway Research, Vol. 10, No. 2, (2023), 9-18

Iran University of Science and Technology

International Journal of Railway Research

ISSN: 2423-3838

Smart Detection of Wheel Defects Using Artificial Intelligence and Wayside Monitoring System

Araliya Mosleh[1*], Mohammadreza Mohammadi[1], Cecília Vale [1], Diogo Ribeiro[2], Pedro Montenegro[1], Andreia Meixedo[1]

[1]CONSTRUCT – LESE, Faculty of Engineering, University of Porto, Porto, Portugal (amosleh@fe.up.pt)

[1]CONSTRUCT – LESE, Faculty of Engineering, University of Porto, Porto, Portugal (mohammadreza.mohammadi.sm@gmail.com)

[1]CONSTRUCT – LESE, Faculty of Engineering, University of Porto, Porto, Portugal (cvale@fe.up.pt)

[2]CONSTRUCT – LESE, School of Engineering, Polytechnic of Porto, Porto, Portugal (drr@isep.ipp.pt)

[1]CONSTRUCT – LESE, Faculty of Engineering, University of Porto, Porto, Portugal (paires@fe.up.pt)

[1]CONSTRUCT – LESE, Faculty of Engineering, University of Porto, Porto, Portugal (ameixedo@fe.up.pt)

ARTICLE INFO

Article history:
Received: 07.12.2023
Accepted: 10.10.2023
Published: 10.14.2023

Keywords:
artificial intelligence
damage detection
wheel flat
train-track dynamic interaction
wayside condition monitoring

A B S T R A C T

Given the significant role of the railway sector in transportation, railway managers and operators place great importance on traffic and maintenance costs. While existing track wayside monitoring systems can detect geometric defects in train wheels, like flats, they do not provide a severity assessment. To address this limitation, the WAY4SafeRail project aims to enhance rail safety by assessing the condition of train wheels. As an initial step in employing Artificial Intelligence Techniques, this paper presents a portion of the research conducted within the WAY4SafeRail project, specifically focusing on numerical simulations of wheel defects, in particular wheel flats. The proposed methodology has demonstrated its reliability and cost-effectiveness in identifying wheel defects.

1. Introduction

Wheel flats result from the friction occurring between the wheel and the rail on railway vehicles [1]. If a wheel flat occurs, it could potentially damage the bogie mechanism, affecting the vehicle's stability during operation and overall riding comfort [2]. As a result, it is essential to conduct corrective maintenance when wheel flats occur. Typically, railway maintenance personnel inspect wheel flats visually, one by one. However, consider a standard train consisting of 10 units; this illustrates the challenge of inspecting 80 wheels individually.

Furthermore, relying solely on visual inspections often results in missed wheel flats and continued operation of damaged wheels. Consequently, this approach diminishes work efficiency and shortens the wheelset's lifespan. To address this issue, it becomes imperative to implement condition-based maintenance, enhancing work efficiency and prolonging wheel lifespan. Additionally, railway vehicles incur maintenance costs of hundreds of millions of dollars annually. Therefore, the systematic

* Corresponding author
Email address: amosleh@fe.up.pt

[DOI: 10.22068/ijrare.322]

application of condition-based maintenance is expected to reduce overall life cycle costs [3].

Randall [4] conducted a study on vibration signals originating from both rotating and reciprocating machinery, including abnormal signals identified during analysis. Gao et al. [5] introduced a technique for diagnosing wheel flat defects in rail vehicles, which relied on detecting vertical changes caused by these defects using the Parallelogram Mechanism. Liang et al. [6] applied time-frequency methods to detect wheel flats, while Yang et al. [7] successfully employed supervised learning to identify rail defects. Chandra et al. [8] used unsupervised learning to detect rail clamp defects. Bosso et al. [9] devised a method to detect wheel flat defects by measuring vertical acceleration on the axle box, with validation through simulations and testing. Initially, the wheel flat index algorithm could detect small flats and estimate their severity. Mosleh et al. [10, 11] proposed a method to differentiate between a defective and healthy wheel based on the envelope spectrum technique.

In recent decades, various onboard and wayside systems have been suggested for detecting wheel defects during train operations [12, 13]. Several onboard technologies utilize vibration, acoustics, image detection, and ultrasonics [9]. Achieving a complete diagnosis of wheel conditions and effective management necessitates equipping all wheels with sensors. However, this approach is infrequently employed due to its high cost and maintenance challenges. As an alternative, wayside measurement systems are employed to identify wheel flats because they assess all wheels as trains pass [2, 14, 15].

While numerous publications have addressed railway defect detection, the available literature on automatic early wheel flat detection is, to the authors' knowledge, quite scarce. Most of the proposed wheel flat detection techniques do not possess the capability to automatically differentiate a defective wheel from a healthy one. Moreover, the majority of the studies mentioned above rely on multiple sensors to make this distinction. This research introduces an automatic method for detecting wheel flats using an unsupervised learning approach, utilizing just a single sensor installed on the rail.

The current paper presents a segment of the research conducted within the WAY4SafeRail project, specifically focusing on numerical simulations of wheel defects. The primary objectives of this project are twofold: firstly, to enhance the assessment of railway wheel conditions during operation by monitoring and categorizing the severity of wheel issues, and secondly, to improve the safety of vehicle operations by detecting instability situations, such as unbalanced loads and the hunting movement, through the application of robust artificial intelligence techniques to measurement data. A notable advantage of this methodology lies in its capacity to increase railway track availability and lifespan while simultaneously reducing maintenance costs. The proposed approach has proven to be a dependable and cost-efficient means of identifying wheel defects.

2. Numerical modeling

2.1. Modeling of vehicle

The present research investigates the Laagrss freight train, which comprises five wagons. According to the UIC classification, this train is capable of reaching a maximum speed of 120 km/h [16]. Figure 1 represents a double freight wagon with a weight of 27 t and a carrying capacity of 52 t. To create a 3-D multibody dynamic model that accounts for suspensions in all directions, ANSYS® [18] is employed. This model employs spring-damper and mass-point elements to represent mass and inertia at the center of gravity for each wagon component and connects these components using rigid beams. The mechanical and geometric properties of the vehicle are summarized in Table 1. Further details regarding the numerical model of the freight wagons can be found in the work of Bragança et al. [19].

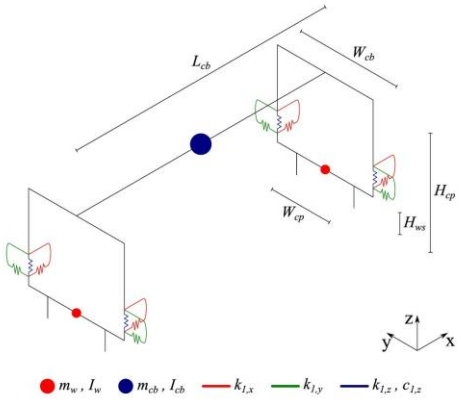

Figure 1. Modeling of the vehicle

[DOI: 10.22068/ijrare.322]

Table 1. Mechanical and geometric properties of the vehicle

Parameter	Symbol (unit)	Adopted value
Carbody		
Mass	m_{cb} (t)	41.1
Roll moment of inertia	$I_{cb,x}$ (t.m^2)	49
Pitch moment of inertia	$I_{cb,y}$ (t.m^2)	673
Yaw moment of inertia	$I_{cb,z}$ (t.m^2)	665
Length	L_{cb} (m)	10000
Wheelset		
Mass	m_w (kg)	1247
Roll moment of inertia	$I_{w,x}$ (kg.m^2)	312
Yaw moment of inertia	$I_{w,z}$ (kg.m^2)	312
Suspensions		
Longitudinal stiffness	$k_{1,x}$ (kN/m)	44981
Lateral stiffness	$k_{1,y}$ (kN/m)	30948
Vertical stiffness	$k_{1,z}$ (kN/m)	1860
Vertical damping	$c_{1,z}$ (kN.s/m)	16.7

2.2. Modeling of the track

Montenegro et al. [20] have developed a finite element model of the track using ANSYS® [18]. Figure 2 illustrates this model, replicating the ballast, sleepers, and rails through a multi-layer approach. The railpads, positioned between the sleepers and the rail, are represented as spring elements that connect the sleepers and the rail. Beam elements depict the rails and sleepers, with suitable material properties assigned to each. Discrete mass points represent the ballast. Additionally, to consider foundation flexibility, spring-dashpot elements are integrated. Table 2 provides a description of the track model, while further details about the numerical model of freight wagons can be found in Mosleh et al. [10].

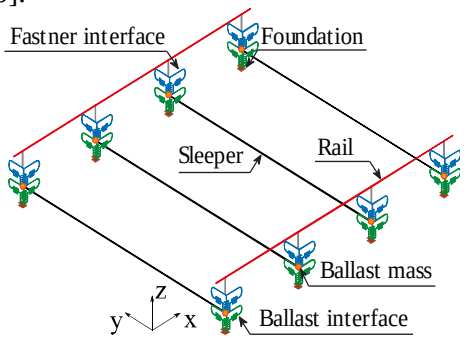

Figure 2. Modeling of the track

Table 2. Mechanical properties of the track

Parameter	Symbol (Unit)	Value
Rail	A_r (m^2)	7.67×10^{-4}
	ρ_r (kg.m^3)	7850
	I_r (m^4)	30.38×10^{-6}
	E_r (N/m^2)	210×10^9
Rail pad, longitudinal	$k_{p,x}$ (N/m)	20×10^6
	$C_{p,x}$ (N.s/m)	50×10^3
Rail pad, lateral	$k_{p,y}$ (N/m)	20×10^6
	$C_{p,y}$ (N.s/m)	50×10^3
Rail pad, vertical	$k_{p,z}$ (N/m)	500×10^6
	$C_{p,z}$ (N.s/m)	200×10^3
Sleeper	ρ_s (N/m)	2590
Ballast, longitudinal	$k_{b,x}$ (N/m)	900×10^3
	$C_{b,x}$ (N.s/m)	15×10^3
Ballast, lateral	$k_{b,y}$ (N/m)	2250×10^3
	$C_{b,y}$ (N.s/m)	15×10^3
Ballast, vertical	$k_{b,z}$ (N/m)	30×10^6
	$C_{b,z}$ (N.s/m)	15×10^3
Foundation, longitudinal	$k_{f,x}$ (N/m)	20×10^6
Foundation, lateral	$k_{f,y}$ (N/m)	20×10^6
Foundation, vertical	$k_{f,z}$ (N/m)	20×10^6

2.3. Track irregularity

Actual railway tracks exhibit minor imperfections in their rails. Despite the small scale of these irregularities, their impact on the interaction between wheels and rails should not be underestimated [21]. Consequently, rail unevenness profiles are created within wavelength ranges from 1 m to 75 m, aligning with the D1 and D2 wavelength intervals defined in the European Standard EN 13848-2 [22]. Additionally, Power Spectral Density (PSD) curves are formulated based on real-world data to generate artificial unevenness profiles. For further details on how these unevenness profiles are generated, please refer to Mosleh et al. [15].

2.4. Wheel flat profile

In this study, the second wheel of the third wagon on the left side is designated as a defective wheel. A uniform statistical distribution examines various combinations of flat wheel depths (D) and flat wheel lengths (L). Three categories are considered for defective wheels with different flat lengths (L): low (L1),

[DOI: 10.22068/ijrare.322]

medium (L2), and severe (L3). The lower and upper limits of the wheel flat length for each interval are determined by the uniform distributions U (10, 20), U (25, 50), and U (55, 100). The wheel flat depth (D) is calculated using the following equation:

$$D = \frac{L^2}{16R_w} \quad (1)$$

In addition, the vertical profile of a wheel flat is determined as follows, where Rw represents the wheel's radius, and L denotes the length of the flat:

$$Z = -\frac{D}{2}\left(1 - \cos\frac{2\pi x}{L}\right).H\left(x - (2\pi R_w - L)\right),$$
$$0 \le x \le 2\pi R_w \quad (2)$$

2.5. Train track interaction

To replicate the dynamic interactions between trains and tracks, the authors have developed a proprietary software known as VSI - Vehicle-Structure Interaction Analysis. This software's validation and comprehensive description are available in prior publications [23], where it has been applied in various contexts [11, 20]. Employing a 3D wheel-rail contact model, the normal contact forces are computed using Hertzian theory, while the tangential forces arising from rolling friction creep are determined using the USETAB routine. MATLAB® [17] serves as the numerical tool for importing the structural matrices of vehicles and tracks, which were previously modeled via finite element analysis (FE). In ANSYS® [18], as previously explained, both subsystems are initially modeled separately, and the VSI software combines them using a fully coupled approach (see [23]). Further details regarding the interaction between the train and track can be found in the authors' prior publications [10, 11, 24, 25]. Figure 3 illustrates the numerical model. Wheel flat detection is achieved by installing eight accelerometers along the track, with four sensors on the right side and four sensors on the left side, all positioned on the rail between two sleepers.

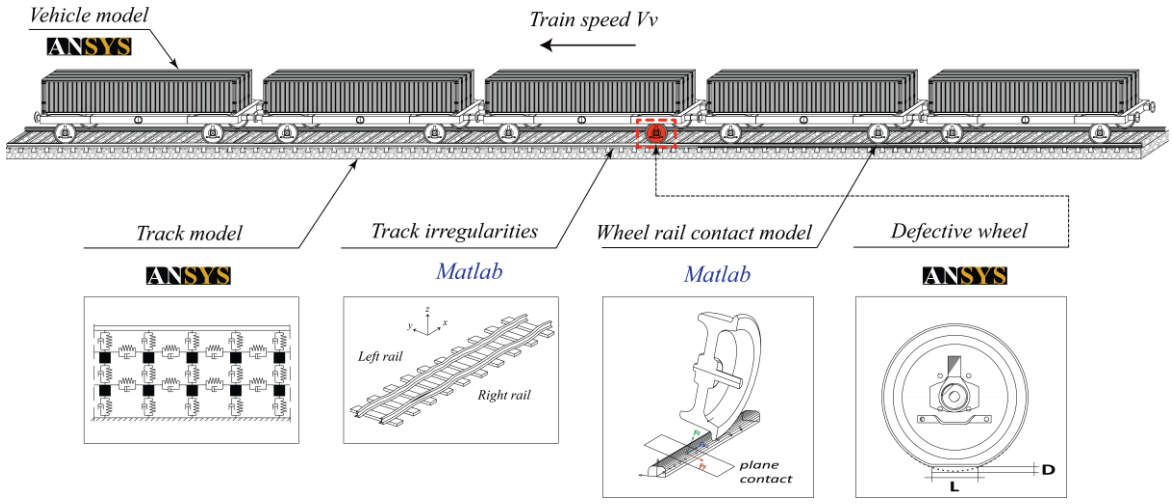

Figure 3. Train-track system

2.6. Damaged and undamaged scenarios

In the context of the current study, two scenarios are examined to test and validate the automatic wheel flat detection method: undamaged (baseline) wheels and damaged wheels. The baseline scenario simulates a train passage with wheels in healthy condition, while the damaged scenario simulates a train passage with defective wheels. Table 3 provides details on the assumptions and the number of numerical simulations for each scenario.

For the baseline scenarios, a total of 113 simulations are conducted for a freight train composed of five wagons. Six different loading scenarios are considered, including (i) an empty train, (ii) a half-loaded train, (iii) a fully loaded train, and trains with unbalanced loads denoted as UNB1, UNB2, and UNB3. Various unbalanced loading configurations are described in the UIC loading guidelines [16], involving longitudinal and transverse offsets of the cargo's center of gravity. Furthermore, 30 simulations are carried out for the damaged scenarios,

[DOI: 10.22068/ijrare.322]

encompassing different flat characteristics. Within each flat length interval (L1, L2, and L3), ten analyses are performed while the train travels at a speed of 80 km/h.

Table 3. Damaged and undamaged scenarios

	Baseline scenario	Damaged scenario
Train	Freight – Laagrss wagon	
Number of loading schemes	6	1 (full capacity)
Unevenness profiles	4	1
Speeds (km/h)	40 – 120	80
Noise ratio	5%	
Flat lengths (mm)	-	10-20 mm (L1) 25-50 mm (L2) 55-100 mm (L3)
Number of numerical analysis	100	30

3. Proposed methodology for automatic wheel flat detection

This methodology, designed for the automated detection of wheel flats [26, 27], operates through a sequence of five steps outlined in Figure 4:

1- Sensors provide input signals for detecting wheel defects.

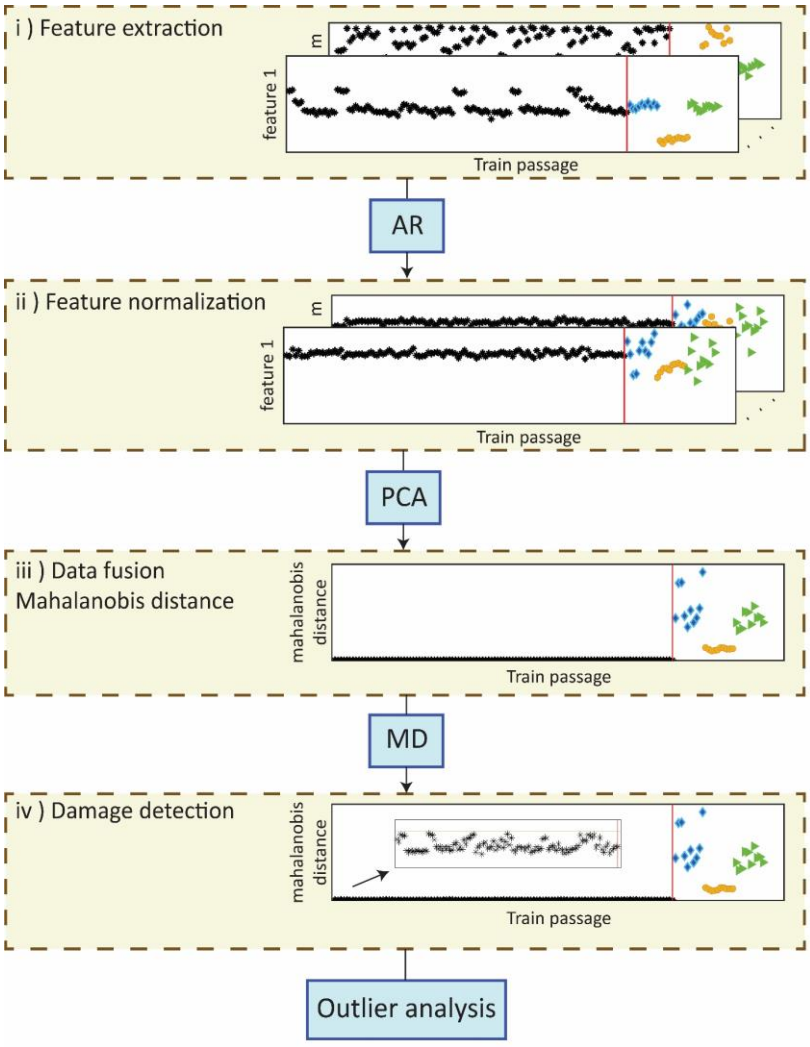

Figure 4. Proposed methodology for damage detection.

[DOI: 10.22068/ijrare.322]

2- The Autoregressive (AR) model is utilized for feature extraction from multiple sensors. During this phase, time series measurements are transformed into features that are sensitive to damage, resulting in significant data compression.

3- The extracted features are subsequently normalized using the Principal Component Analysis (PCA) technique to eliminate operational variations and heighten their sensitivity to damage.

4- Additionally, the Mahalanobis distance (MD) is applied to the modeled features to amplify the sensitivity to the damage further. This distance metric facilitates the effective fusion of features from each sensor, resulting in the generation of a damage indicator (DI) for each train passage.

5- Finally, a statistical approach is employed to determine whether a wheel is in a healthy or defective condition. Leveraging a Gaussian Inverse Cumulative Distribution Function, a statistical Confidence Boundary (CB) is estimated.

4. Results and discussion

4.1. Feature extraction

In this study, the extraction of features is carried out by implementing the Autoregressive (AR) model. A total of 40 AR parameters are calculated from the time series data collected by each accelerometer using the Akaike Information Criterion (AIC) technique and subsequently employed as features sensitive to damage. The application of the AR model to the 143 scenarios results in the creation of three-dimensional matrices sized at 143-by-40-by-8. The features can be categorized into two main groups, distinguishing between the condition of the train's wheels: baseline scenarios, encompassing the first 113 passages, and damaged scenarios, which include the following 30 passages. Each damage scenario, indicative of wheel flat severity (ranging from low to high), is represented by ten indicators.

Consequently, simulations numbered from 114 to 123 pertain to vehicle passages with wheel flat lengths spanning from 10 to 20 mm (L1), while simulations 124 to 133 relate to vehicle passages featuring wheel flat lengths between 25 and 50 mm (L2). Wheel flat lengths within the range of 55 to 100 mm (L3) are considered in simulations 134 to 143. The diversity of information present in various AR parameters is depicted in Figure 5. For instance, Figure 5a identifies a specific sensitivity pattern for damaged scenarios, rendering the amplitude distinctions between scenarios with low, moderate, and severe damage discernible. In both baseline and damage scenarios (as depicted in Figure 5b), features with higher values exhibit reduced amplitude variations compared to those with lower values. Typically, the differentiation between baseline and damage scenarios is not straightforward due to the influence of environmental and operational factors. Hence, the subsequent section introduces the implementation of feature normalization.

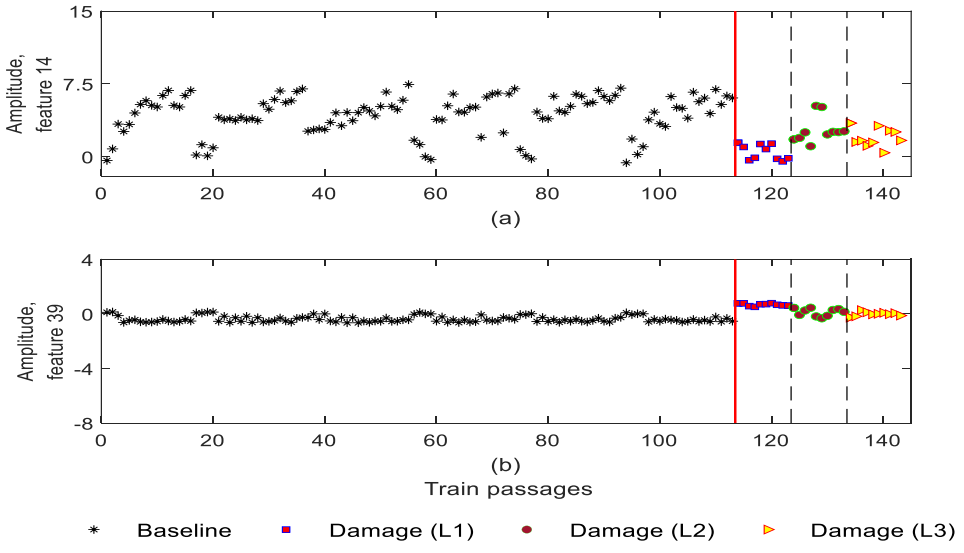

Figure 5. Feature extraction

* Corresponding author
Email address: amosleh@fe.up.pt

[DOI: 10.22068/ijrare.322]

4.2. Feature normalization

Enhancing the clarity of damage detection entails the removal of environmental and operational influences from the responses. Therefore, a matrix of features for each vehicle passage is generated using PCA and relies on AR parameters. The first two components are eliminated during the modeling phase due to the cumulative variance exceeding 80%. Figure 6 represents two PCA features out of the 40 available for each of the 143 scenarios, encompassing both undamaged and damaged scenarios. Given the limited distinctions between undamaged and damaged scenarios, the differentiation between a healthy and defective wheel becomes impractical following PCA implementation. Consequently, the subsequent section proceeds with data fusion.

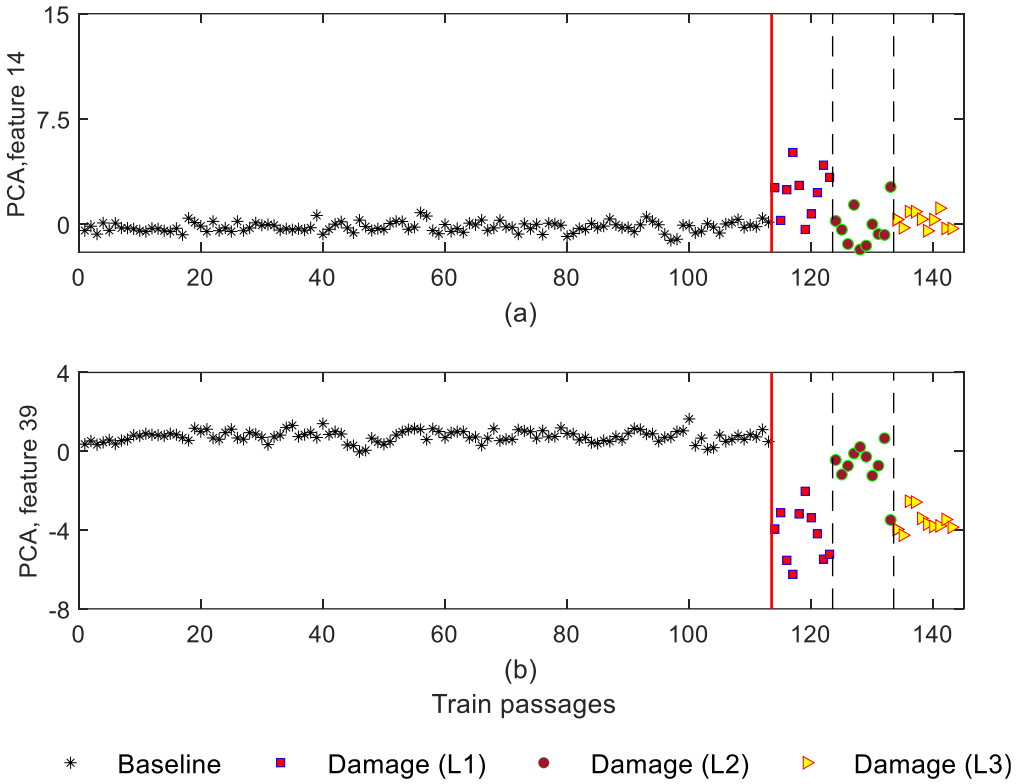

Figure 6. Feature normalization

4.3. Data fusion

A damage index (DI) is formulated by merging features through the utilization of Mahalanobis distance (MD). MD assesses the degree of similarity between undamaged and damaged features based on their respective distances, with shorter distances signifying a higher level of similarity. Through MD, each sensor and vehicle passage are transformed into a damage-sensitive feature using the 40 AR-PCA parameters. This process yields vectors of distances measuring 143 by 1 for each of the 8 sensors. Figure 7 visually illustrates the distinct improvements in sensitivity exhibited by different sensors. Additionally, the figure highlights the varying degrees of sensitivity to damage across sensors, creating diverse damage indexes.

4.4. Automatic wheel flat detection

In the final step, as depicted in Figure 4, the proposed methodology performs automatic wheel flat detection by utilizing a Gaussian inverse cumulative distribution function to calculate a confidence boundary (CB). A threshold with a significance level of 1% is employed. Figure 8 illustrates the automated

* Corresponding author
Email address: amosleh@fe.up.pt

[DOI: 10.22068/ijrare.322]

damage detection outcomes for all 143-wheel conditions. The results in this figure demonstrate that the proposed method is exceptionally proficient in distinguishing between a healthy wheel and a defective one, achieving this without any false positives or false negatives.

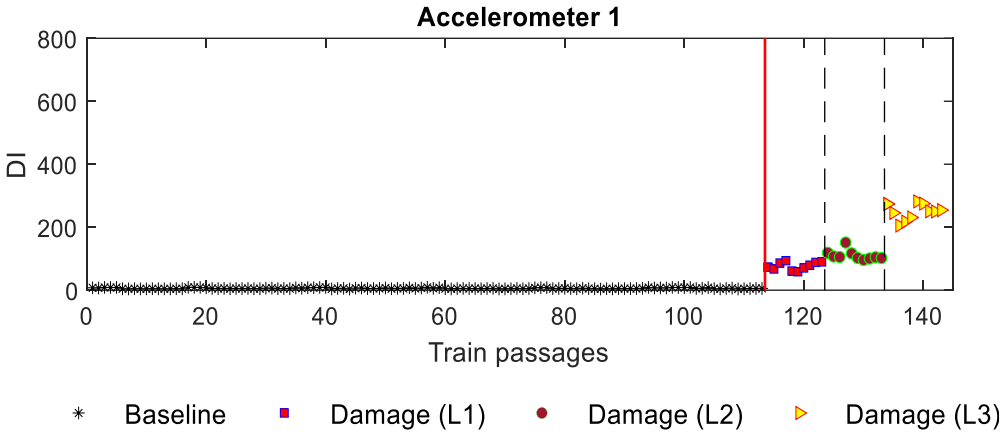

Figure 7. Data fusion

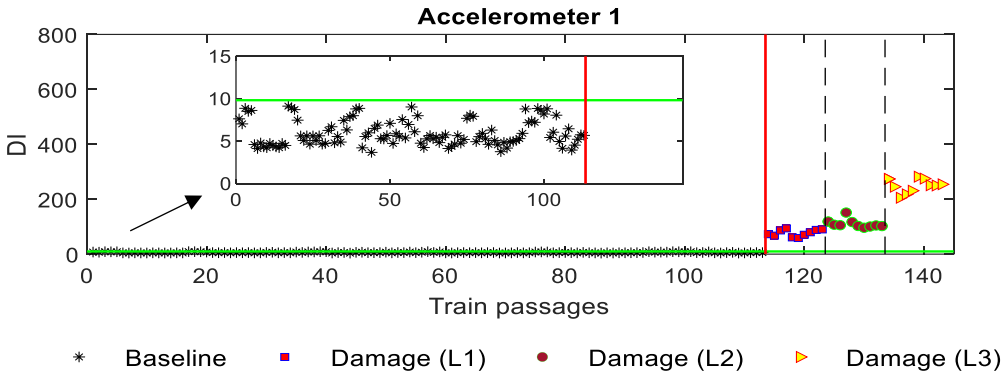

Figure 8. Automatic wheel flat detection

5. Conclusion

The objective of developing an unsupervised damage detection methodology is to automatically differentiate between a defective train wheel and a healthy one. The proposed methodology encompasses the following steps: (i) data acquisition through installed sensors; (ii) feature extraction from the acquired responses; (iii) feature normalization to mitigate environmental and operational variations; (iv) data fusion to consolidate features while preserving wheel defect information; and (v) feature classification to categorize the extracted features into two groups: a healthy wheel or a defective one. Baseline and damage scenarios were created by manipulating input parameters such as train type, train loads and speeds, rail irregularity profile, and various wheel flat depth and length combinations. Notably, the methodology accomplished this task without a single false detection, effectively distinguishing a healthy wheel from a defective one, irrespective of the train type, rail irregularities, or train speed. Furthermore, using just one sensor proved sufficient for detecting a defective wheel. Future work will entail a field trial further to assess the practical utility of the developed technology.

[DOI: 10.22068/ijrare.322]

Declaration of Conflicting Interests

The author(s) declared no potential conflicts of interest with respect to the research, authorship, and/or publication of this article.

Acknowledgements

The paper reflects research developed in the ambit of the project Way4SafeRail, NORTE-01-0247-FEDER-069595, founded by Agência Nacional de Inovação S.A., program P2020|COMPETE—Projetos em Copromoção. The first author acknowledges Grant no. 2021.04272.CEECIND from the Stimulus of Scientific Employment, Individual Support (CEECIND) - 4rd Edition provided by "FCT – Fundação para a Ciência INTERNATIONAL JOURNAL OF RAIL TRANSPORTATION23e Tecnologia".

References

[1] V. Gonçalves, A. Mosleh, C. Vale,P.A. Montenegro, Wheel Out-of-Roundness Detection Using an Envelope Spectrum Analysis. Sensors, 2023. 23(4): p. 2138.

[2] A. Guedes, R. Silva, D. Ribeiro, C. Vale, A. Mosleh, P. Montenegro,A. Meixedo, Detection of Wheel Polygonization Based on Wayside Monitoring and Artificial Intelligence. Sensors, 2023. 23(4): p. 2188.

[3] R. Silva, A. Guedes, D. Ribeiro, C. Vale, A. Meixedo, A. Mosleh,P. Montenegro, Early Identification of Unbalanced Freight Traffic Loads Based on Wayside Monitoring and Artificial Intelligence. Sensors, 2023. 23(3): p. 1544.

[4] R.B. Randall, State of the art in monitoring rotating machinery-part 1. Sound and vibration, 2004. 38(3): p. 14-21.

[5] R. Gao, Q. He,Q. Feng, Railway wheel flat detection system based on a parallelogram mechanism. Sensors, 2019. 19(16): p. 3614.

[6] B. Liang, S. Iwnicki, G. Feng, A. Ball, V.T. Tran,R. Cattley, Railway wheel flat and rail surface defect detection by time-frequency analysis. CHEMICAL ENGINEERING, 2013. 33.

[7] C. Yang, Y. Sun, C. Ladubec,Y. Liu, Developing machine learning-based models for railway inspection. Applied Sciences, 2020. 11(1): p. 13.

[8] P. Chandran, F. Thiery, J. Odelius, H. Lind,M. Rantatalo, Unsupervised Machine Learning for Missing Clamp Detection from an In-Service Train Using Differential Eddy Current Sensor. Sustainability, 2022. 14(2): p. 1035.

[9] N. Bosso, A. Gugliotta,N. Zampieri, Wheel flat detection algorithm for onboard diagnostic. Measurement, 2018. 123: p. 193-202.

[10] A. Mosleh, P. Montenegro, P. Alves Costa,R. Calçada, An approach for wheel flat detection of railway train wheels using envelope spectrum analysis. Structure and Infrastructure Engineering, 2021. 17(12): p. 1710-1729.

[11] A. Mosleh, P.A. Montenegro, P.A. Costa,R. Calçada, Railway Vehicle Wheel Flat Detection with Multiple Records Using Spectral Kurtosis Analysis. Applied Sciences, 2021. 11(9): p. 4002.

[12] A. Mosleh, A. Meixedo, D. Ribeiro, P. Montenegro,R. Calçada, Early wheel flat detection: an automatic data-driven wavelet-based approach for railways. Vehicle System Dynamics, 2022: p. 1-30.

[13] J.C.O. Nielsen,A. Johansson, Out-of-round railway wheels-a literature survey. Proceedings of the Institution of Mechanical Engineers, Part F: Journal of Rail and Rapid Transit, 2000. 214(2): p. 79-91.

[14] A. Amini, M. Entezami, Z. Huang, H. Rowshandel,M. Papaelias, Wayside detection of faults in railway axle bearings using time spectral kurtosis analysis on high-frequency acoustic emission signals. Advances in Mechanical Engineering, 2016. 8(11): p. 1687814016676000.

[15] A. Mosleh, P.A. Costa,R. Calçada, A new strategy to estimate static loads for the dynamic weighing in motion of railway vehicles. Proceedings of the Institution of Mechanical Engineers, Part F: Journal of Rail and Rapid Transit, 2019. 234(2): p. 183-200.

[16] UIC, Code of practice for the loading and securing of goods on railway wagons. 2022: Paris.

[17] M. MATLAB®. Natick, USA: Release R2018a, The MathWorks Inc. 2018: Natick, Massachusetts: The MathWorks Inc.

[18] ANSYS®. 2018 C, Academic Research: C, PA, USA.

[19] C. Bragança, J. Neto, N. Pinto, P.A. Montenegro, D. Ribeiro, H. Carvalho,R. Calçada, Calibration and validation of a freight wagon dynamic model in operating conditions

[DOI: 10.22068/ijrare.322]

based on limited experimental data. Vehicle System Dynamics, 2022. 60(9): p. 3024-3050.
[20] P.A. Montenegro, R. Heleno, H. Carvalho, R. Calçada,C.J. Baker, A comparative study on the running safety of trains subjected to crosswinds simulated with different wind models. Journal of Wind Engineering and Industrial Aerodynamics, 2020. 207: p. 104398.
[21] V.C.C. R. Dynamic Response of a Coupled Vehicle-Track System to Real Longitudinal Rail Profiles. in Proceedings of the Tenth International Conference on Computational Structures Technology, Civil-Comp Press. 2010. Stirlingshire, UK.
[22] E. STANDARD, Railway applications - Track - Track geometry quality - Part 2: Measuring systems - Track recording vehicles (EN 13848-2). 2006: Brussels: EUROPEAN COMMITTEE FOR STANDARDIZATION.
[23] P.A. Montenegro, S.G.M. Neves, R. Calçada, M. Tanabe,M. Sogabe, Wheel–rail contact formulation for analyzing the lateral train–structure dynamic interaction. Computers & Structures, 2015. 152: p. 200-214.
[24] M. Mohammadi, A. Mosleh, C. Vale, D. Ribeiro, P. Montenegro,A. Meixedo, An Unsupervised Learning Approach for Wayside Train Wheel Flat Detection. Sensors, 2023. 23(4): p. 1910.
[25] A. Mosleh, P.A. Montenegro, P.A. Costa,R. Calçada, Approaches for weigh-in-motion and wheel defect detection of railway vehicles, in Rail Infrastructure Resilience. 2022, Elsevier. p. 183-207.
[26] A. Mosleh, A. Meixedo, D. Ribeiro, P. Montenegro,R. Calçada, Automatic clustering-based approach for train wheels condition monitoring. International Journal of Rail Transportation, 2022: p. 1-26.
[27] A. Meixedo, J. Santos, D. Ribeiro, R. Calçada,M. Todd, Online unsupervised detection of structural changes using train–induced dynamic responses. Mechanical Systems and Signal Processing, 2022. 165: p. 108268, doi:10.1016/j.ymssp.2021.108268.

[DOI: 10.22068/ijrare.322]